

# Forward-backward multiplicity correlations in relativistic heavy-ion collisions in a superposition approach

Adam Olszewski<sup>1,\*</sup> and Wojciech Broniowski<sup>1,2,†</sup>

<sup>1</sup>*Institute of Physics, Jan Kochanowski University, PL-25406 Kielce, Poland*

<sup>2</sup>*The H. Niewodniczański Institute of Nuclear Physics,  
Polish Academy of Sciences, PL-31342 Kraków, Poland*

(Dated: 21 March 2013)

We analyze the multiplicity correlations between distant forward and backward rapidity regions in relativistic heavy-ion collisions in a superposition framework, where the particle production occurs through independent emission from correlated sources. This allows for inferring information on the long-range forward-backward correlations of the sources in the earliest phase of the collision, based on the experimental information on the statistical features of the observed particle distributions. Our three-stage study incorporates the fluctuations of parton production in the early phase, the effect of intermediate hydrodynamic evolution, as well as fluctuations in the production of particles at freeze-out. We investigate the dependence of the results on the features of the overlaid distributions and hydrodynamics, as well as the centrality dependence. We confirm the previous conclusions of the substantial forward-backward event-by-event fluctuation of sources implied by the data from the STAR Collaboration. Predictions based of the Glauber model of the initial phase for the forward-backward multiplicity correlations in Pb+Pb collisions at the LHC are made.

PACS numbers: 25.75.-q, 25.75.Gz, 25.75.Ld

Keywords: relativistic heavy-ion collisions, LHC, RHIC, forward-backward correlations

## I. INTRODUCTION

The forward-backward (FB) multiplicity correlations in relativistic heavy-ion collisions, recently measured at RHIC [1–4], were followed with a number of theoretical studies [5–19]. The primary goal of these analyses is to get insight into the space-time dynamics of the earliest stages of the reaction, probed via the long-range correlations. A simplified statistical understanding [5, 6, 14] of the problem is gained when one considers initially formed *sources* (wounded nucleons [20–22], possibly amended with binary collisions [23, 24], Glasma [25–28], dual strings [5, 29]), which later lead to particle production occurring *independently* (and with the same distribution) from each source. Such *superposition models* lead to simple relations between the statistical features (moments, correlations) of the distributions of sources and of the produced particles, which involve properties of the overlaid distribution as parameters [5, 14].

In this paper we analyze in detail the predictions of this framework, tailoring it closely to the popular description of the relativistic heavy-ion dynamics based on three stages: initial phase, hydrodynamics, and statistical hadronization (for a review see, e.g., [30]). The key assumption is that the emission from a source is universal, i.e., occurs from the same statistical distribution independently of the centrality class of the collision. This leads to very simple formulas for the statistical measures, in particular for the correlation coefficient between the

numbers of particles produced in the forward and backward rapidity bins. Parameters in these relations depend on the features of the overlaid statistical distributions and the properties of hydrodynamics.

We use the derived relations in two ways. First, using the experimental data from the STAR Collaboration [2–4] for the correlation and the scaled variance, we obtain an expression for the correlation of sources in the early phase, involving one free parameter dependent on the unknown features of the overlaid distributions and hydrodynamics. This straightforwardly generalizes the treatment of Brogueira and Dias de Deus [5] and Białas, Bzdak, and Zalewski [14], who use a Poisson distribution in the two-step approach. We confirm the conclusions of Ref. [14] of the possible large hidden event-by-event asymmetry in the distribution of sources in the RHIC setup. We carry out our analysis for the Au+Au and Cu+Cu collisions at  $\sqrt{s_{NN}} = 200$  GeV, where the data are available.

Second, we use the relations in the opposite direction, starting from the properties of the source distribution and computing the FB correlation of the produced particles. We use the Glauber framework for this purpose. Predictions, involving one free parameter, for the Pb+Pb collisions at  $\sqrt{s_{NN}} = 2.76$  TeV at the Large Hadron Collider (LHC) are made that way. We predict a decrease of the FB correlations of particles with centrality, which follows from the decrease of the scaled variance of the sources. The future data from the LHC will verify this scenario.

The outline of the paper is as follows: In section (II) we briefly recall the three-stage approach, consisting of the early production, the hydrodynamic evolution, and the final freezeout. We then derive the basic relations linking the statistical features of the sources and of the final

\* Adam.Olszewski.Fiz@gmail.com

† Wojciech.Broniowski@ifj.edu.pl

particle distributions. In Sec. (III) we use the data from the STAR Collaboration for the Au+Au and Cu+Cu collisions to obtain the FB multiplicity correlations of the sources. Finally, in Sec. (IV) we present our predictions for the FB correlations of particle multiplicities to be experimentally analyzed with the LHC for the Pb+Pb system. We use the approach introduced in Sec. (II) and the distributions of sources obtained with the mixed model [23, 24] from GLISSANDO [31].

## II. THREE-STAGE APPROACH

Much of success in the description of the relativistic heavy-ion dynamics has been achieved in a three-stage model (for a review see, e.g., [30]), consisting of

1. Early production, modeled in terms of the Glauber approach [20–24, 32], Glasma [25–28], string formation [5, 29], etc.
2. Hydrodynamic evolution, starting from the initial condition provided by stage 1 (for reviews see, e.g., [30, 33, 34], and for the recent event-by-event studies [35–44]).
3. Statistical hadronization, carried out at freezeout right after the hydrodynamic phase ends, e.g., [45–56].

The approach leads to a proper description of such measured quantities as multiplicities, spectra, harmonic flow coefficients, femtoscopic properties, etc., [57], thus is viewed as a practical framework. Statistical fluctuations are generated in phases 1 and 3, while phase 2 is assumed to be deterministic (although one may include fluctuations also in this phase [58]). Of course, the most interesting are the fluctuations in the initial stage, as they refer to the important physics at the earliest times and may help to discriminate between various physics approaches, while the fluctuations at hadronization form a “statistical noise” which should be disposed of. While each of the stages is physically involved, including numerous physical parameters, and needless to say, takes a huge effort to simulate numerically, certain statistical aspects, as we shall see, can be understood and classified in rather simple terms, displaying the possible scenarios in the FB correlations of the earliest phase.

Throughout this paper we use the generic concept of *sources*, which may be viewed statistically as the density of partons (or fields) in the initial phase, turning into the entropy density of the fluid cell in the hydrodynamic phase, which in the end, at freeze-out, gives birth to the observed hadrons streaming to the detectors. In the context of the FB multiplicity fluctuations, an important assumption is the sufficient kinematic separation of the forward (F) and backward (B) rapidity windows, such that the particles produced in from the F source do not fall into the B window, and vice versa. This allows us

to trace the evolution of a cell with fluctuating sources. Suppose in the early-production phase we separate the F and B cells in spatial rapidity, with the original number of sources  $s$  denoted as  $s_F$  and  $s_B$ , respectively. These numbers fluctuate event-by-event and may be correlated, which is what we eventually want to assess. In the initial production mechanism these sources produce partons  $p$ , whose density supplies the initial condition for hydrodynamics.

Assuming that the production occurs from each source in the same manner, we then have

$$p_A = \sum_{i=1}^{s_A} \mu_i, \quad A = F, B, \quad (1)$$

where the random variable  $\mu_i$  is the number of partons produced from the source  $i$ . As mentioned, we assume that the distribution of  $\mu_i$  is universal, i.e., does not depend on the location of the cell, and that the production from different cells is *independent* from one another. Then the formulas for the superposition model follow (see Appendix A):

$$\begin{aligned} \langle p_A \rangle &= \langle \mu \rangle \langle s_A \rangle, \\ \text{var}(p_A) &= \text{var}(\mu) \langle s_A \rangle + \langle \mu \rangle^2 \text{var}(s_A), \\ \text{cov}(p_F, p_B) &= \langle \mu \rangle^2 \text{cov}(s_F, s_B), \end{aligned} \quad (2)$$

where  $A = F, B$ .

The sources  $p$  yield the entropy density which constitutes an event-by-event initial condition for the collective evolution via hydrodynamics. The hydrodynamic evolution is dynamically complicated, however, it is deterministic. Thus the evolution of the cell with initially  $p$  sources yields  $h$  sources at freeze-out ( $p$  and  $h$  may be thought of as entropy contained in the cell), where  $h$  is a function of  $p$ .<sup>1</sup> The phase-space location of the fluid cells is evolved due to the hydrodynamic push, however, the separation between the far-lying F and B regions is maintained. If the event-by-event fluctuations are not too large, we may expand

$$h = t_0 \langle p \rangle + t_1 (p - \langle p \rangle) + \mathcal{O}((p - \langle p \rangle)^2), \quad (3)$$

where  $t_i$  are parameters depending on dynamical properties of hydrodynamics. The higher-order terms may be dropped if  $p$  is sufficiently close to  $\langle p \rangle$ . The constant term is written in the form  $t_0 \langle p \rangle$ . Then

$$\begin{aligned} \langle h_A \rangle &= t_0 \langle p_A \rangle, \\ \text{var}(h_A) &= t_1^2 \text{var}(p_A), \\ \text{cov}(h_F, h_B) &= t_1^2 \text{cov}(p_F, p_B). \end{aligned} \quad (4)$$

---

<sup>1</sup> Strictly speaking, the hydrodynamic evolution depends not only on the number of sources  $p$ , but also on their spatial distribution, hence the same values of  $p$  may lead to somewhat different  $h$ . Such nuances can only be included in a fully numerical simulation. We do not expect them to be relevant for our analysis.

Equation (3) requires some discussion. If the response of hydrodynamics is such that  $h \sim t$ , i.e. the entropy in the considered cell after the evolution is proportional to the initial entropy, then  $t_0 \simeq t_1$ . The success of hydrodynamics in reproducing the rapidity spectra starting from an initial Glauber condition (see, e.g., [59]) supports this scenario. Moreover, it suggests that  $t_0$  and  $t_1$  are independent of centrality in the range of applicability of hydrodynamics. Secondly, since in viscous hydrodynamics the entropy is produced, we have in a given cell  $\langle h \rangle > \langle p \rangle$ , which implies  $t_0 > 1$ . The production of entropy depends on the properties of hydrodynamics, but is not very large [59] (25-50%), such that we expect  $t_0$  to be only somewhat larger than 1. To summarize, we arrive at the estimates

$$\begin{aligned} t_0 &\simeq t_1 \sim 1, \\ t_0 &> 1. \end{aligned} \quad (5)$$

The parameters  $t_0$  and  $t_1$  should be treated as specific to a given reaction or rapidity bin, but independent of centrality.

Finally, statistical hadronization is carried out at freezeout. We assume that a given cell emits  $n$  hadrons into a region of phase-space with some statistical distribution superimposed over  $h$ . Similarly to the analogous mechanism in the initial phase, each of the  $h$  sources emits independently  $m$  hadrons with the same distribution. In reality some mixing may occur and particles may be emitted from different cells into the same kinematic region. However, if the F and B cells are well separated, this effect is negligible. Thus we have

$$n_A = \sum_{i=1}^{h_A} m_i, \quad (6)$$

and

$$\begin{aligned} \langle n_A \rangle &= \langle m \rangle \langle h_A \rangle, \\ \text{var}(n_A) &= \text{var}(m) \langle h_A \rangle + \langle m \rangle^2 \text{var}(h_A). \\ \text{cov}(n_F, n_B) &= \langle m \rangle^2 \text{cov}(h_F, h_B). \end{aligned} \quad (7)$$

The three-stage model and the notation introduced above may be summarized with the following diagram:

$$s \xrightarrow{\text{init. production}} p \xrightarrow{\text{hydro}} h \xrightarrow{\text{hadronization}} n$$

Joining Eqs. (2-7) yields

$$\begin{aligned} \langle n_A \rangle &= \alpha \langle s_A \rangle, \\ \text{var}(n_A) &= \beta \langle s_A \rangle + \gamma \text{var}(s_A), \\ \text{cov}(n_F, n_B) &= \gamma \text{cov}(s_F, s_B). \end{aligned} \quad (8)$$

where the combinations of constants are

$$\begin{aligned} \alpha &= t_0 \langle \mu \rangle \langle m \rangle, \\ \beta &= t_0 \langle \mu \rangle \text{var}(m) + t_1^2 \langle m \rangle^2 \text{var}(\mu), \\ \gamma &= t_1^2 \langle \mu \rangle^2 \langle m \rangle^2. \end{aligned} \quad (9)$$

It is convenient to introduce the scaled variance  $\omega(x_A) = \text{var}(x_A)/\langle x_A \rangle$  and the correlation coefficients  $\rho(x_F, x_B) = \text{cov}(x_F, x_B)/(\sigma(x_F)\sigma(x_B))$ . Then, for symmetrically separated bins where  $\sigma(x_F) = \sigma(x_B)$ , we can write the relations

$$\begin{aligned} \omega(n_A) &= \delta + \kappa \omega(s_A), \\ \rho(n_F, n_B) &= \frac{\rho(s_F, s_B)}{1 + \lambda/\omega(s_A)}, \end{aligned} \quad (10)$$

with

$$\begin{aligned} \delta &= \beta/\alpha = \omega(m) + \frac{t_1^2}{t_0} \langle m \rangle \omega(\mu), \\ \kappa &= \gamma/\alpha = \frac{t_1^2}{t_0} \langle \mu \rangle \langle m \rangle, \\ \lambda &= \beta/\gamma = \frac{t_0 \omega(m)}{t_1^2 \langle \mu \rangle \langle m \rangle} + \frac{\omega(\mu)}{\langle \mu \rangle}. \end{aligned} \quad (11)$$

Formulas (8,10) express the statistical properties of the event-by-event distributions of the produced particles in the F and B bins via the properties of the distribution of the original sources. Note that the relation between the correlation coefficients depends on a single combination of the unknown parameters of the overlaid distributions and hydrodynamics represented in  $\lambda$ , which makes the qualitative analysis simple.<sup>2</sup>

We may also write the reversed formulas expressing the properties of the initial sources through the properties of the final particle distributions:

$$\begin{aligned} \langle s_A \rangle &= \frac{1}{\alpha} \langle n_A \rangle, \\ \omega(s_A) &= \frac{\omega(n_A)}{\kappa} - \lambda, \\ \rho(s_F, s_B) &= \frac{\rho(n_F, n_B)}{1 - \delta/\omega(n_A)}. \end{aligned} \quad (12)$$

A feature following from the assumptions in our analysis is the independence of the parameters  $\alpha$ ,  $\beta$ ,  $\gamma$ ,  $\delta$ ,  $\kappa$ , and  $\lambda$  on the centrality class. This dependence resides entirely in the statistical properties of the distributions of  $s$  or  $n$ .

Finally, we note that the inclusion of finite experimental acceptance  $a$  amounts to overlaying yet another statistical distribution over  $n$ , with mean  $a$  and variance  $a(1-a)$ . As a result, the parameters  $\alpha$ ,  $\beta$ , and  $\gamma$  are changed, however, the form of Eqs. (8-12) remains unaltered.

The basic methodology is as follows: Eq. (12) involves three independent parameters:  $\alpha$ ,  $\kappa$ , and  $\lambda$  (note that  $\delta = \kappa\lambda$ ). Thus, knowing from the experiment  $\langle n_A \rangle$ ,  $\omega(n_A)$ , and  $\rho(n_F, n_B)$  and from the model  $\langle s_A \rangle$ ,  $\omega(s_A)$ , and  $\rho(s_F, s_B)$  (at a given centrality) allows us to solve

<sup>2</sup> This feature is a derivative of the form of Eq. (3). Note also that overlaying more distributions preserves the form of Eq. (8,10).

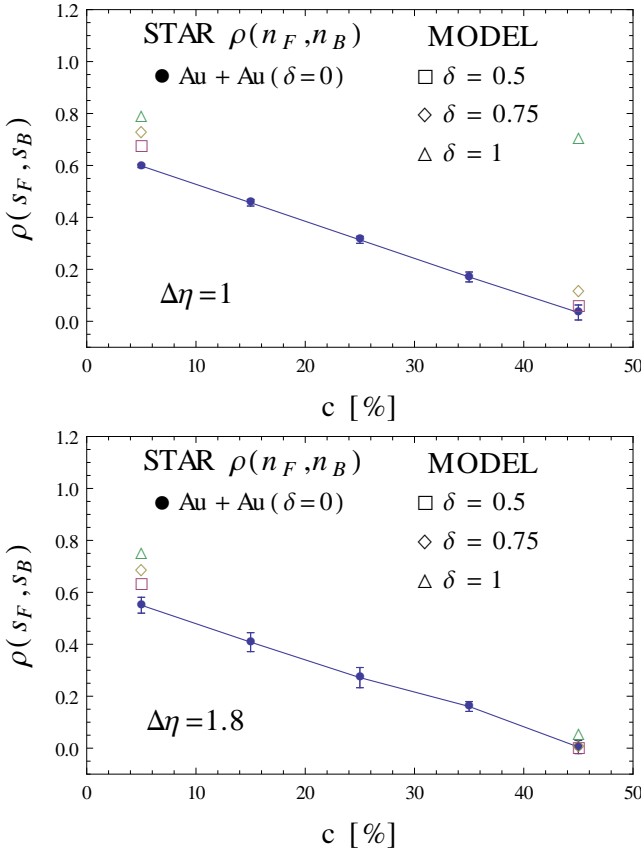


FIG. 1. (Color online) Forward-backward correlation of the initial sources in Au+Au collisions inferred from the STAR data [3, 4], plotted as a function of centrality for several values of the  $\delta$  parameter in Eq. (12). The case  $\delta = 0$  (joined with the line) corresponds to the STAR data for  $\rho(n_F, n_B)$ .

the equations for  $\alpha$ ,  $\kappa$ , and  $\lambda$ . Comparing the values at various centralities serves as a consistency check.<sup>3</sup> For this program to be feasible, one needs the complete experimental data involving  $\langle n_A \rangle$ ,  $\omega(n_A)$ , and  $\rho(n_F, n_B)$  at all centralities, which, unfortunately, is not the case of Refs. [3, 4], where  $\omega(n_A)$  is provided only for two centrality classes. For that reason the above program is carried out only partially in the following Sections. On the model side, we need  $\langle s_A \rangle$ ,  $\omega(s_A)$ , and  $\rho(s_F, s_B)$ .

### III. ANALYSIS OF THE STAR DATA

We now use Eq. (12) and the data from the STAR Collaboration [3, 4] for the Au+Au and Cu+Cu collisions at RHIC at the energy  $\sqrt{s_{NN}} = 200$  GeV to compute the correlation of sources  $\rho(s_F, s_B)$ . We use here the data

<sup>3</sup> More appropriately, one should simultaneously solve the equations at all centralities in the  $\chi^2$  sense.

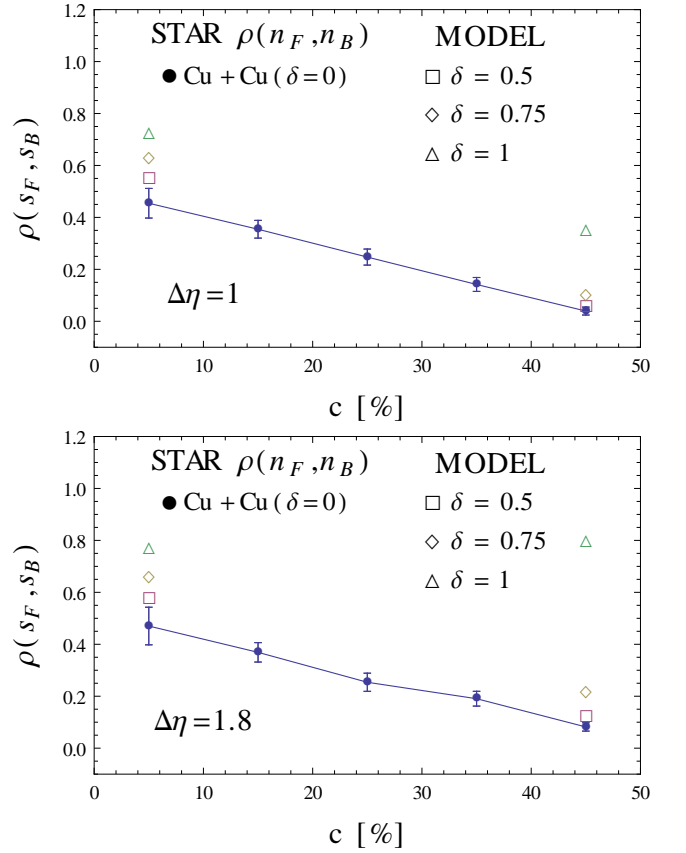


FIG. 2. (Color online) Same as Fig. 1 for the Cu+Cu collisions.

for the the well-separated symmetric bins at  $\Delta\eta = 1$  and  $\Delta\eta = 1.8$ . As already mentioned, the experimental variance  $\text{var}(s_A)$ , necessary for the analysis in Eq. (12), is provided only for two centrality bins: 0-10% and 40-50%. The values of  $\langle s_A \rangle$  at various centralities are read off from Fig. 4.1 of [3].

The results are shown in Figs. 1 and 2, where the FB correlations of the initial sources in the Au+Au and Cu+Cu collisions is plotted as a function of centrality for several values of the  $\delta$  parameter of Eq. (12). The case  $\delta = 0$  corresponds to the STAR data for  $\rho(n_F, n_B)$ . Naturally, increasing  $\delta$  leads to larger  $\rho(s_F, s_B)$ . We cannot use too large values of  $\delta$ , as  $\rho(s_F, s_B) \leq 1$  and, as follows from Eq. (12),

$$\delta \leq \omega(n_A)[1 - \rho(n_F, n_B)]. \quad (13)$$

Numerically, it gives the maximum allowed values for  $\delta$  at  $c = 0 - 10\%$  equal to 1.6 and 1.3 for Au+Au and Cu+Cu, respectively, while at  $c = 40 - 50\%$  the maximum values are only slightly larger than 1. Insisting on the independence of  $\delta$  on centrality, we find (from the STAR data for  $c = 40 - 50\%$ ) that  $\delta \simeq 1$  saturates the bound (13).

We note that the value  $\delta = 1$  and the corresponding  $\rho(s_F, s_B) \simeq 0.8$  for the Au+Au case,  $c = 0 - 10\%$ , is

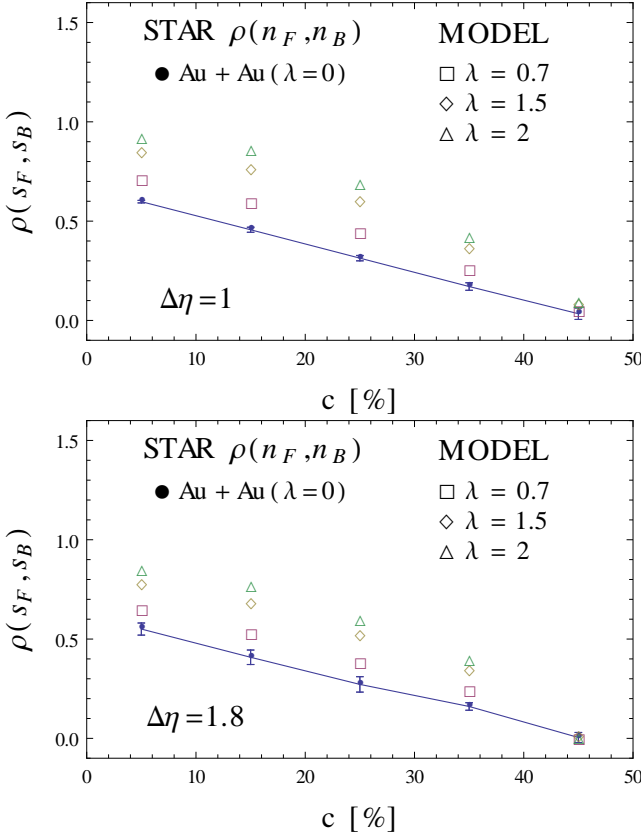


FIG. 3. (Color online) Forward-backward correlation of the initial sources in Au+Au collisions obtained from Eq. (10) with various values of  $\lambda$ .

consistent with the number obtained in Ref. [14], where (in the notation of that paper)

$$\frac{D_-}{D_+} = \sqrt{\frac{\langle (s_F - s_B)^2 \rangle}{\langle (s_F + s_B)^2 \rangle}} = \sqrt{\frac{1 - \rho(s_F, s_B)}{1 + \rho(s_F, s_B)}} \simeq \frac{1}{3}. \quad (14)$$

This means that the fluctuations of the sources are quite substantially decorrelated, i.e.,  $\rho(s_F, s_B)$  is less than 1.

We may now use the value of  $\delta$  to obtain information on the underlying parameters of the overlaid distributions and hydrodynamics. From Eq. (11) it follows that  $\omega(m) + \frac{t^2}{t_0} \langle m \rangle \omega(\mu) \simeq 1$ . The weak bound deduced from here is that the distribution of  $m$  cannot be wider than Poissonian, i.e.,  $\omega(m) \leq 1$ .

Above, we have used exclusively the experimental information to conclude the dependence of  $\rho(s_F, s_B)$  on centrality, which is possible only for the two bins where the experimental values of  $\omega(n_A)$  are provided. We now fill the missing points by using some information from the Glauber model as well. For that purpose we rewrite Eq. (10) in the form

$$\rho(s_F, s_B) = \rho(n_F, n_B)(1 + \lambda/\omega(s_A)), \quad (15)$$

where on the right-hand side we use the experimental data for the correlation coefficient and the mixed

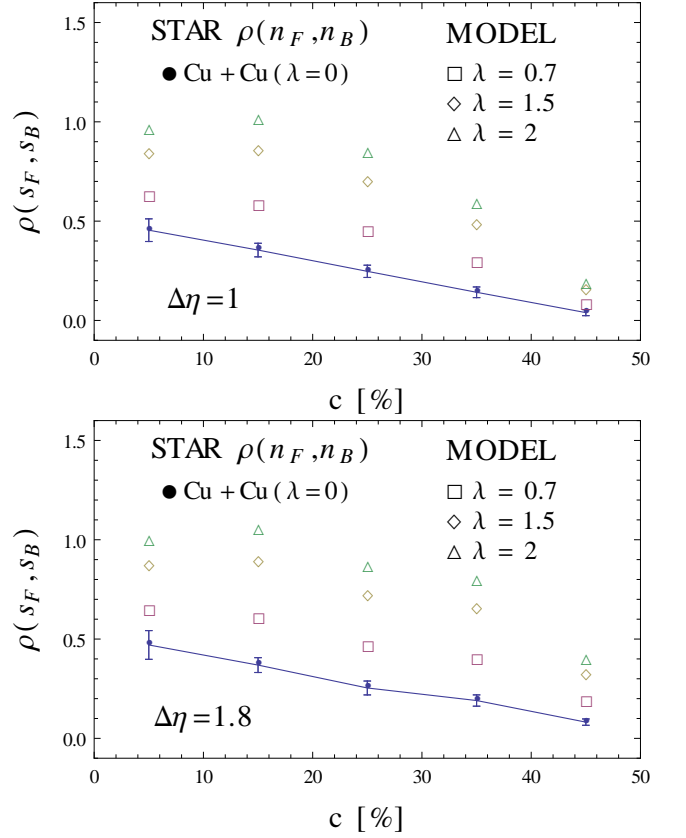


FIG. 4. (Color online) Same as Fig. 3 for the Cu+Cu collisions.

Glauber model [31] result for  $\omega(s_A)$ . For the RHIC energies  $\sqrt{s_{NN}} = 200$  GeV we take the mixing parameter  $\alpha = 14.5\%$  and  $\sigma_{NN} = 42$  mb. The results of our procedure are shown in Fig. 3-4.

The main conclusion of this section is a gradual decrease of  $\rho(s_F, s_B)$  with centrality, which, as enforced by the data, drops to nearly zero at  $c = 40 - 50\%$ . The effect occurs for both the Au+Au and Cu+Cu reactions.

We note that the first measurements of the FB multiplicity correlations at RHIC were carried out by the PHOBOS collaboration [1]. Since the statistical measure used in that work is different from the correlation coefficient, we do not use the PHOBOS data in the present analysis.

#### IV. PREDICTIONS FOR THE LHC

Finally, we use Eq. (10) to predict the FB correlation for the Pb+Pb collisions at the collision energy of  $\sqrt{s_{NN}} = 2.76$  TeV at the LHC. The values of  $\omega(s_A)$  are obtained from the mixed model Glauber implemented in GLISSANDO. In particular, we take the mixing parameter  $\alpha = 15\%$  and  $\sigma_{NN} = 67$  mb. Figure (5) shows our predictions, which will be verified when the LHC data for

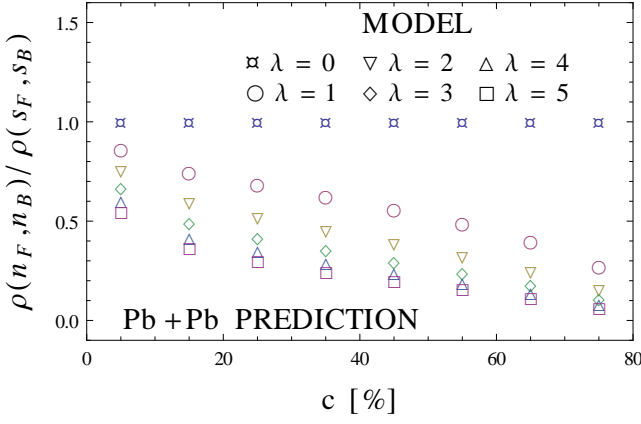


FIG. 5. (Color online) Predictions for the ratio of the FB multiplicity correlation of measured particles to the FB correlation of sources, plotted as a function of centrality, obtained from Eq. (15) at different values of  $\lambda$ . The scaled variance  $\omega(s_A)$  is taken from GLISSANDO for the mixed model. The simulation is for the Pb+Pb collisions at the LHC energy of  $\sqrt{s_{NN}} = 2.76$  TeV.

the FB multiplicity correlations are analyzed. We note a gradual fall-off of  $\rho(n_F, n_B) / \rho(s_F, s_B)$  with centrality. This fall-off is due to the fact that the scaled variance  $\omega(s_A)$  decreases with growing centrality. We note that the fall-off in Fig. 5 is much weaker than in the STAR data in Figs. 1, 2, in particular at  $c = 40 - 50\%$  the points in Fig. 5 assume about a half of the central values.

## V. CONCLUSIONS

In this paper we have extended the analysis of correlations in superposition models, previously made in Refs. [5, 6, 14], to the case of the three-stage approach consisting of the early production, hydrodynamics, and statistical hadronization. Simple formulas, linking the statistical properties of the FB correlations in the data and in the original sources have been derived. The effect of hydrodynamics may be, under reasonable assumptions, incorporated in terms of just two parameters independent of centrality. The relations between the FB multiplicity correlations of the produced particles and the initial sources involve a single parameter, which collects the features of the overlaid distributions and hydrodynamics. These one-parameter formulas allow to verify the model of the production early phase with the experiment, under the proviso that the data are sufficiently complete in providing, for each centrality, not only the FB correlation coefficient, but also the variance of the number of particles in the F and B bins.

We have confirmed the findings of Ref. [14] that the STAR data [3, 4] suggest a substantial degree of decorrelation of the sources in the F and B bins, which means large event-by-event FB fluctuations in multiplicity. A

similar feature is seen in the Cu-Cu data.

The awaited FB correlation analysis with the LHC data will shed further light on the early production mechanism. The statistical method presented in this paper is directly applicable to that case. We argue that the complete data consisting of the average multiplicity and variance in the forward and backward rapidity bins, as well as the forward-backward correlation coefficient, will allow for a verification of production models of the early phase.

This research was supported by the Polish National Science Centre, grant DEC-2011/01/D/ST2/00772.

## Appendix A: Superposition model

In this Appendix we derive the relevant statistical formulas. Let the number of produced particles  $n$  be composed of independent emissions from  $s$  sources,

$$n = \sum_{i=1}^s m_i. \quad (A1)$$

Here  $m_i$  is the number of particles produced by the  $i$ th source from some universal distribution. Then the well-known relations follow:

$$\langle n \rangle = \langle s \rangle \langle m \rangle, \quad (A2)$$

$$\text{var}(n) = \langle s \rangle \text{var}(m) + \langle m \rangle^2 \text{var}(s). \quad (A3)$$

We give for completeness the derivation. Introduce

$$\delta m_i = m_i - \langle m \rangle, \quad \text{with } \langle \delta m_i \rangle = 0. \quad (A4)$$

Then

$$\begin{aligned} \text{var}(n) &= \left\langle \left( \sum_{i=1}^s (\delta m_i + \langle m \rangle) \right)^2 \right\rangle - (\langle s \rangle \langle m \rangle)^2 \\ &= \left\langle \sum_{i=1}^s \delta m_i^2 \right\rangle + \left\langle \sum_{i,j=1, i \neq j}^s \delta m_i \delta m_j \right\rangle + 2 \langle m \rangle \left\langle \sum_{i=1}^s \delta m_i \right\rangle \\ &\quad + \langle m \rangle^2 \left\langle \left( \sum_{i=1}^s \sum_{j=1}^s \delta m_i \delta m_j \right) \right\rangle - \langle s \rangle^2 \langle m \rangle^2. \end{aligned} \quad (A5)$$

The second and third term in the last equality vanish due to Eq. (A4). Also, from the independence of the production from different sources, the first term is equal to  $\langle s \rangle \text{var}(m)$ . Finally, using the obvious fact that  $\sum_{i=1}^s \sum_{j=1}^s \delta m_i \delta m_j = s^2$  we obtain Eq. (A3).

Next, we look at the covariance between two well-separated bins, which means  $\langle m_i m_j \rangle = \langle m \rangle^2$ , with  $i$  and  $j$  belonging to two different bins. We have

$$\langle n_1 n_2 \rangle = \left\langle \sum_{i=1}^{s_1} m_i \sum_{j=1}^{s_2} m_j \right\rangle = \langle m \rangle^2 \langle s_1 s_2 \rangle, \quad (A6)$$

and

For the correlation coefficient it follows that

$$\rho(n_1, n_2) = \frac{\rho(s_1, s_2)}{\sqrt{1 + \frac{\omega(m)}{\langle m \rangle \omega(s_1)}} \sqrt{1 + \frac{\omega(m)}{\langle m \rangle \omega(s_2)}}}. \quad (\text{A8})$$

$$\text{cov}(n_1, n_2) = \langle m \rangle^2 \text{cov}(s_1, s_2). \quad (\text{A7})$$

- 
- [1] B. Back *et al.* (PHOBOS Collaboration), Phys.Rev. **C74**, 011901 (2006), arXiv:nucl-ex/0603026 [nucl-ex].
- [2] T. J. Tarnowsky (STAR Collaboration), (2006), arXiv:nucl-ex/0606018 [nucl-ex].
- [3] T. J. Tarnowsky, (2008), arXiv:0807.1941 [nucl-ex].
- [4] B. Abelev *et al.* (STAR Collaboration), Phys.Rev.Lett. **103**, 172301 (2009), arXiv:0905.0237 [nucl-ex].
- [5] P. Brogueira and J. Dias de Deus, Phys.Lett. **B653**, 202 (2007), arXiv:hep-ph/0611329 [hep-ph].
- [6] P. Brogueira, J. Dias de Deus, and J. G. Milhano, Phys.Rev. **C76**, 064901 (2007), arXiv:0709.3913 [hep-ph].
- [7] S. Haussler, M. Abdel-Aziz, and M. Bleicher, Nucl.Phys. **A785**, 253 (2007), arXiv:nucl-th/0608021 [nucl-th].
- [8] A. Bzdak and K. Wozniak, Phys.Rev. **C81**, 034908 (2010), arXiv:0911.4696 [hep-ph].
- [9] A. Bzdak, Phys.Rev. **C80**, 024906 (2009), arXiv:0902.2639 [hep-ph].
- [10] Y.-L. Yan, D.-M. Zhou, B.-G. Dong, X.-M. Li, H.-L. Ma, *et al.*, Phys.Rev. **C81**, 044914 (2010), arXiv:1001.1595 [nucl-th].
- [11] T. Lappi and L. McLerran, Nucl.Phys. **A832**, 330 (2010), arXiv:0909.0428 [hep-ph].
- [12] T. Lappi, Int.J.Mod.Phys. **E20**, 1 (2011), arXiv:1003.1852 [hep-ph].
- [13] A. Bialas and K. Zalewski, Phys.Rev. **C82**, 034911 (2010), arXiv:1008.4690 [hep-ph].
- [14] A. Bialas, A. Bzdak, and K. Zalewski, Phys.Lett. **B710**, 332 (2012), arXiv:1107.1215 [hep-ph].
- [15] A. Bialas and K. Zalewski, Phys.Lett. **B698**, 416 (2011), arXiv:1101.5706 [hep-ph].
- [16] A. Bialas and K. Zalewski, Nucl.Phys. **A860**, 56 (2011), arXiv:1101.1907 [hep-ph].
- [17] A. Bzdak, Phys.Rev. **C85**, 051901 (2012), arXiv:1108.0882 [hep-ph].
- [18] A. Bzdak and D. Teaney, (2012), arXiv:1210.1965 [nucl-th].
- [19] K. Fialkowski and R. Wit, Central Eur.J.Phys. **10**, 1125 (2012), arXiv:1203.3671 [nucl-th].
- [20] A. Bialas, M. Bleszynski, and W. Czyz, Nucl.Phys. **B111**, 461 (1976).
- [21] A. Bialas, J.Phys. **G35**, 044053 (2008).
- [22] W. Broniowski, P. Bozek, and M. Rybczynski, Phys.Rev. **C76**, 054905 (2007), arXiv:0706.4266 [nucl-th].
- [23] D. Kharzeev and M. Nardi, Phys.Lett. **B507**, 121 (2001), arXiv:nucl-th/0012025 [nucl-th].
- [24] B. Back *et al.* (PHOBOS Collaboration), Phys.Rev. **C65**, 031901 (2002), arXiv:nucl-ex/0105011 [nucl-ex].
- [25] A. Kovner, L. D. McLerran, and H. Weigert, Phys.Rev. **D52**, 6231 (1995), arXiv:hep-ph/9502289 [hep-ph].
- [26] E. Iancu, A. Leonidov, and L. D. McLerran, Nucl.Phys. **A692**, 583 (2001), arXiv:hep-ph/0011241 [hep-ph].
- [27] T. Lappi, Prog.Theor.Phys.Suppl. **187**, 134 (2011), arXiv:1011.0821 [hep-ph].
- [28] T. Lappi, J.Phys.Conf.Ser. **270**, 012055 (2011).
- [29] N. Amelin, N. Armesto, M. Braun, E. Ferreira, and C. Pajares, Phys.Rev.Lett. **73**, 2813 (1994).
- [30] W. Florkowski, *Phenomenology of Ultra-Relativistic Heavy-Ion Collisions* (World Scientific Publishing Company, Singapore, 2010).
- [31] W. Broniowski, M. Rybczynski, and P. Bozek, Comput.Phys.Commun. **180**, 69 (2009), arXiv:0710.5731 [nucl-th].
- [32] W. Czyz and L. Maximon, Annals Phys. **52**, 59 (1969).
- [33] P. F. Kolb and U. W. Heinz, in *Quark Gluon Plasma 3*, edited by R. Hwa and X. N. Wang (World Scientific, Singapore, 2004) arXiv:nucl-th/0305084.
- [34] P. Huovinen and P. V. Ruuskanen, Ann. Rev. Nucl. Part. Sci. **56**, 163 (2006), arXiv:nucl-th/0605008.
- [35] R. Andrade, F. Grassi, Y. Hama, T. Kodama, and J. Socolowski, O., Phys. Rev. Lett. **97**, 202302 (2006), nucl-th/0608067.
- [36] K. Werner *et al.*, J. Phys. **G36**, 064030 (2009), arXiv:0907.5529 [nucl-th].
- [37] H. Petersen, G.-Y. Qin, S. A. Bass, and B. Muller, Phys.Rev. **C82**, 041901 (2010), arXiv:1008.0625 [nucl-th].
- [38] H. Holopainen, H. Niemi, and K. J. Eskola, Phys.Rev. **C83**, 034901 (2011), arXiv:1007.0368 [hep-ph].
- [39] F. G. Gardim, F. Grassi, M. Luzum, and J.-Y. Ollitrault, (2011), arXiv:1111.6538 [nucl-th].
- [40] P. Bozek, Phys.Rev. **C85**, 014911 (2012), arXiv:1112.0915 [hep-ph].
- [41] B. Schenke, S. Jeon, and C. Gale, Phys. Rev. Lett. **106**, 042301 (2011), arXiv:1009.3244 [hep-ph].
- [42] Z. Qiu and U. W. Heinz, (2011), arXiv:1108.1714 [nucl-th].
- [43] A. Chaudhuri, (2011), arXiv:1112.1166 [nucl-th].
- [44] P. Bozek and W. Broniowski, Phys.Rev.Lett. **109**, 062301 (2012), arXiv:1204.3580 [nucl-th].
- [45] F. Cooper and G. Frye, Phys. Rev. **D10**, 186 (1974).
- [46] P. Braun-Munzinger, D. Magestro, K. Redlich, and J. Stachel, Phys.Lett. **B518**, 41 (2001), arXiv:hep-ph/0105229 [hep-ph].

- [47] W. Broniowski and W. Florkowski, Phys.Rev.Lett. **87**, 272302 (2001), arXiv:nucl-th/0106050 [nucl-th].
- [48] G. Torrieri and J. Rafelski, Phys.Rev. **C68**, 034912 (2003), arXiv:nucl-th/0212091 [nucl-th].
- [49] J. Rafelski and J. Letessier, Acta Phys.Polon. **B34**, 5791 (2003), arXiv:hep-ph/0309030 [hep-ph].
- [50] F. Becattini, M. Gazdzicki, A. Keranen, J. Manninen, and R. Stock, Phys.Rev. **C69**, 024905 (2004), arXiv:hep-ph/0310049 [hep-ph].
- [51] G. Torrieri, S. Steinke, W. Broniowski, W. Florkowski, J. Letessier, *et al.*, Comput.Phys.Commun. **167**, 229 (2005), arXiv:nucl-th/0404083 [nucl-th].
- [52] S. Wheaton and J. Cleymans, Comput.Phys.Commun. **180**, 84 (2009), arXiv:hep-ph/0407174 [hep-ph].
- [53] A. Kisiel, T. Tałuć, W. Broniowski, and W. Florkowski, Comput. Phys. Commun. **174**, 669 (2006), arXiv:nucl-th/0504047.
- [54] N. Amelin, R. Lednicky, T. Pocheptsov, I. Lokhtin, L. Malinina, *et al.*, Phys.Rev. **C74**, 064901 (2006), arXiv:nucl-th/0608057 [nucl-th].
- [55] B. Tomasik, Comput.Phys.Commun. **180**, 1642 (2009), arXiv:0806.4770 [nucl-th].
- [56] M. Chojnacki, A. Kisiel, W. Florkowski, and W. Broniowski, Comput. Phys. Commun. **183**, 746 (2012), arXiv:1102.0273 [nucl-th].
- [57] W. Broniowski, M. Chojnacki, W. Florkowski, and A. Kisiel, Phys.Rev.Lett. **101**, 022301 (2008), arXiv:0801.4361 [nucl-th].
- [58] J. Kapusta, B. Muller, and M. Stephanov, Phys.Rev. **C85**, 054906 (2012), arXiv:1112.6405 [nucl-th].
- [59] P. Bozek, Phys.Rev. **C85**, 034901 (2012), arXiv:1110.6742 [nucl-th].